A Linearized Power Flow Model for Optimization in Unbalanced Distribution Systems

Michael D. Sankur, Roel Dobbe, Emma Stewart, Duncan S. Callaway, and Daniel B. Arnold

***Abstract*— Optimal Power Flow (OPF) is an important tool used to coordinate assets in electric power systems to ensure customer voltages are within pre-defined tolerances and to improve distribution system operations. While convex relaxations of Optimal Power Flow (OPF) problems have been proposed for both balanced and unbalanced networks, these approaches do not provide universal convexity guarantees and scale inefficiently as network size and the number of constraints increase. To address these issues, we have recently explored a novel linearized OPF formulation for unbalanced distribution systems. Our approach is made possible in part by approximating the ratio of voltages across phases throughout the network. In this work, we generalize the previous formulation to allow arbitrary complex numbers to approximate voltage ratios at different locations in the feeder. Furthermore, we continue the analysis of the linearized OPF via comparison to results obtained through convex relaxations and Semi-Definite Programming (SDP). Simulations of IEEE test feeders show that the proposed formulation produces control decisions that closely approximate those obtained via SDP relaxations. In a specific case, we show that the linearized OPF is capable of solving certain problems which cannot be formulated as SDPs.**

I. Introduction

Coordination of a diverse set of Distributed Energy Resources (DER) presents many challenges to utility operators, who strive to ensure power of sufficient quality and quantity is available to retail customers at least cost. Such assets can vary in size from residential rooftop PV units to larger PV arrays and, perhaps, battery storage systems located at residential, commercials and industrial sites. As has been experienced in Hawaii [**?**], the negative impact of high levels of distributed PV under current interconnection standards is significant, and has led to financial impacts to both consumers and the utility. However, distributed generation resources could, under the correct operational control scenarios, provide numerous benefits to the grid, including voltage support, VAR compensation, and ancillary services [**?**].

A variety of strategies for the management of DER presently exist for *balanced* distribution system models. Turitsyn et al. [**?**] considered a suite of distributed control strategies for reactive power compensation using four quadrant inverters. The work of [**?**] studies distributed voltage regulation in the absence of communication, relying on locally obtained information. In [**?**], a two-stage control architecture for voltage regulation is considered where distributed controllers inject power based on local sensitivity measurements. The authors of [**?**] study local voltage reference tracking with integral-type controllers, based on local voltage measurements. The authors of [**?**] address voltage regulation and loss minimization through solving an Optimal Power Flow (OPF) problem, and address convexity issues using second order cone relaxations. The work of [**?**] also considers an OPF approach for voltage regulation in distribution networks by framing the decision-making process as a semidefinite program. The authors provide conditions under which the semidefinite relaxation of the non-convex power flow problem is tight in balanced circuits. It is worth noting that many of the aforementioned approaches can be traced back to the seminal work of [**?**], that introduced nonlinear and linear-approximated recursive branch power flow models.

Approaches to coordinate DER in *unbalanced* distribution systems, while being critical to the practical application in real distribution systems and microgrids [**?**], are much less prevalent in the literature. While there is consensus about the physics-based models [**?**], using these in an optimization setting is challenging. Perhaps the best known efforts have been put forth by Dall'Anese et. al [**?**], [**?**], who consider semidefinite relaxations for OPF problems in unbalanced systems, but do not provide conditions under which feasibility and optimality are guaranteed. In addition to inefficient scaling as the problem size increases, the work of [**?**] points out that it becomes more difficult to find a tight relaxation as the ratio of constraints to network buses increases. A likely reason that more strategies focusing on coordination of distributed energy resources in unbalanced systems do not exist is the lack of suitable linear models that approximate three phase power flow.

In our previous work [**?**], we attempted to fill this void by proposing a linearized unbalanced power flow model that can be viewed as an extension of the *LinDistFlow* [**?**] linear approximation for balanced systems. Using this linear model, we constructed an OPF formulation that dispatched reactive power resources from controllable DER to perform voltage balancing and regulation. In this work, we extend the previously studied model; generalizing it to allow for other linearizations and comparing the results of OPF formulations that employ our linear model to those obtained via convex relaxations and semidefinite programming.

This work has three main contributions. First, we derive a nonlinear model of unbalanced power flow in distribution systems which can be viewed as an extension of the *DistFlow* system of equations, first studied in [**?**]. Secondly, we propose two approximations to linearize the model into a form suitable for incorporation into OPF formulations. Finally, we evaluate the performance of the proposed linearizations numerically. In one experiment, we demonstrate that an OPF driven by our linearized unbalanced power flow model

TABLE I: Nomenclature

V_n^ϕ	Voltage phasor at node n on phase ϕ
$\mathbb{V}_n$	Vector of voltage phasors at node n
y_n^ϕ	Squared magnitude of voltage at node n on phase ϕ
$\mathbb{Y}_n$	Vector of squared magnitudes of voltages at node n
$Z_{mn}^{\phi\psi}$	Impedance of segment (m,n) between phases (ϕ,ψ)
$\mathbb{Z}_{mn}$	Impedance matrix of line segment (m,n)
I_n^ϕ	Current phasor entering node n on phase ϕ
$\mathbb{I}_n$	Vector of current phasors entering node n
i_n^ϕ	Load current of phase ϕ at node n
$\mathbf{i}_n$	Vector of load currents at node n
S_n^ϕ	Phasor of complex power entering node n on phase ϕ
$\mathbb{S}_n$	Vector of complex power phasors entering node n
s_n^ϕ	Load on phase ϕ at node n
$\mathbf{s}_n$	Vector of complex loads at node n
w_n^ϕ	DER complex power dispatch on phase ϕ at node n

produces results that closely approximate those obtained via an OPF that uses convex relaxations. In a second experiment, we compare the proposed linearizations to perform voltage phase balancing and show that an iterative approach can be used to reduce linearization errors.

This work is organized as follows. A derivation of the three phase nonlinear power flow model is presented in Section II, along with two proposed linearization approaches. Section III presents simulation results using the IEEE 13 node test feeder [**?**]. Concluding remarks are provided in Section IV.

II. Analysis

A. Preliminaries

Let $\mathcal{T} = (H, E)$ denote a rooted tree graph representing an unbalanced radial distribution feeder, where H is the set of nodes of the feeder and E is the set of line segments. Nodes are indexed by $i = 0, 1, \ldots, N$, where N is the order (number of nodes) of the distribution feeder, and node 0 denotes the feeder head (or substation). We treat node 0 as an infinite bus, decoupling interactions in the downstream distribution system from the rest of the grid. While the substation voltage may evolve over time, we assume this evolution takes place independently of DER control actions in $\mathcal{T}$. Each line segment can have up to three phases, labeled a, b, and c. For convenience, phases are referred to by the variables ϕ and ψ, where $\phi \in \{a,b,c\}$, $\psi \in \{a,b,c\}$. For adjacent nodes m and n, the current/voltage relationship is captured by Kirchhoff's Voltage and Current Laws (KVL and KCL):

$$\begin{bmatrix} V_m^a \\ V_m^b \\ V_m^c \end{bmatrix} = \begin{bmatrix} V_m^a \\ V_m^b \\ V_m^c \end{bmatrix} + \begin{bmatrix} Z_{mn}^{aa} & Z_{mn}^{ab} & Z_{mn}^{ac} \\ Z_{mn}^{ba} & Z_{mn}^{bb} & Z_{mn}^{bc} \\ Z_{mn}^{ca} & Z_{mn}^{cb} & Z_{mn}^{cc} \end{bmatrix} \begin{bmatrix} I_n^a \\ I_n^b \\ I_n^c \end{bmatrix} \tag{1}$$

$$\begin{bmatrix} I_m^a \\ I_m^b \\ I_m^c \end{bmatrix} = \begin{bmatrix} i_m^a \\ i_m^b \\ i_m^c \end{bmatrix} + \sum_{n:(m,n)\in E} \begin{bmatrix} I_n^a \\ I_n^b \\ I_n^c \end{bmatrix}, \tag{2}$$

where $Z_{mn}^{\phi\psi} = r_{mn}^{\phi\psi} + jx_{mn}^{\phi\psi}$ (with $j = \sqrt{-1}$) denotes the complex impedance of line (m,n) across phases ϕ and ψ. We assume that each node serves a complex load in each phase, $s_m^\phi = V_m^\phi (i_m^\phi)^*$, of the form:

$$s_m^\phi(V_m^\phi) = s_{0,m}^\phi \left(a_{0,m}^\phi + a_{1,m}^\phi |V_m^\phi|^2 \right) + w_m^\phi \tag{3}$$

where $a_{0,m}^\phi + a_{1,m}^\phi = 1$ and are, for simplicity, assumed constant across all phases at each node. The apparent power which can be sourced or sunk by a controllable DER at node m on phase ϕ is denoted by w_m^ϕ. In our convention, positive demand denotes power consumption and negative demand is power injected, or supplied, to the grid. Equations (1)–(3) represent the power flow model that will be used to generate simulations in Section III.

B. Generalized Form: Dist3Flow Equations

We now derive a model of power flow between adjacent buses in an unbalanced distribution system. We begin with writing KVL for an arbitrary line segment (m,n) and KCL at a node m:

$$\mathbb{V}_m = \mathbb{V}_n + \mathbb{Z}_{mn}\mathbb{I}_n \tag{4}$$

$$\mathbb{I}_m = \mathbf{i}_m + \sum_{n:(m,n)\in E} \mathbb{I}_n \tag{5}$$

Right multiplying $\mathbb{V}_m$ by the complex conjugate transpose (denoted by *) of Equation (5) and plugging in (4) on the RHS results in:

$$\begin{aligned} \mathbb{V}_m\mathbb{I}_m^* &= \mathbb{V}_m\mathbf{i}_m^* + \sum_{n:(m,n)\in E} \mathbb{V}_m\mathbb{I}_n^* \\ &= \mathbb{V}_m\mathbf{i}_m^* + \sum_{n:(m,n)\in E} \mathbb{V}_n\mathbb{I}_n^* + \mathbb{Z}_{mn}\mathbb{I}_n\mathbb{I}_n^* \qquad (6) \\ &= \mathbb{V}_m\mathbf{i}_m^* + \sum_{n:(m,n)\in E} \mathbb{V}_n\mathbb{I}_n^* + \mathcal{L}_{mn}, \qquad (7) \end{aligned}$$

where $\mathcal{L}_{mn} = \mathbb{Z}_{mn}\mathbb{I}_n\mathbb{I}_n^* \in \mathbb{C}^{3\times 3}$ denotes the power loss matrix. While (7) is a 3×3 matrix equation, we are only interested in the diagonal entries, which are the complex powers in each phase of the circuit. We collect these entries into a 3×1 vector equation, that yields a relation of the complex power flowing into node m in terms of node m demand, losses in downstream line segments, and powers flowing into downstream nodes:

$$\mathbb{S}_m = \mathbf{s}_m + \sum_{n:(m,n)\in E} \mathbb{S}_n + \mathbb{L}_{mn} \tag{8}$$

where $\mathbb{L}_{mn} \in \mathbb{C}^3$ with $\mathbb{L}_{mn}(i) = \mathcal{L}_{mn}(i,i)$ for $i = 1,2,3$. We now return to KVL on edge $(m,n) \in E$, and right multiply both sides by their respective complex conjugate transpose, yielding the 3×3 matrix equation:

$$\begin{aligned} \mathbb{V}_m\mathbb{V}_m^* &= \mathbb{V}_n\mathbb{V}_n^* + \mathbb{Z}_{mn}\mathbb{I}_n\mathbb{V}_n^* + \mathbb{V}_n\mathbb{I}_n^*\mathbb{Z}_{mn}^* + \mathbb{Z}_{mn}\mathbb{I}_n\mathbb{I}_n^*\mathbb{Z}_{mn}^* \\ &= \mathbb{V}_n\mathbb{V}_n^* + 2\,\mathbf{Re}\left\{\mathbb{V}_n\mathbb{I}_n^*\mathbb{Z}_{mn}^*\right\} + \mathcal{H}_{mn}, \qquad (9) \end{aligned}$$

where $\mathcal{H}_{mn} = \mathbb{Z}_{mn}\mathbb{I}_n\mathbb{I}_n^*\mathbb{Z}_{mn}^* \in \mathbb{C}^{3\times 3}$ denotes the higher order term matrix. Noticing that for the scalar current $(I_n^\phi)^* = S_n^\phi (V_n^\phi)^{-1} \in \mathbb{C}$ we can write (9) as:

$$\begin{aligned} &\mathbb{V}_m\mathbb{V}_m^* = \mathbb{V}_n\mathbb{V}_n^* + \mathcal{H}_{mn} + \ldots \\ &2\,\mathbf{Re}\left\{\mathbb{V}_n \begin{bmatrix} S_n^a(V_n^a)^{-1} & S_n^b(V_n^b)^{-1} & S_n^c(V_n^c)^{-1} \end{bmatrix} \mathbb{Z}_{mn}^*\right\}. \end{aligned} \tag{10}$$

Now, we define $\gamma_n^{\phi,\psi}$ as the ratio of voltages between phases ϕ and ψ at node n, or $\gamma_n^{\phi\psi} = V_n^{\phi}(V_n^{\psi})^{-1}$, where $\phi, \psi \in \{a, b, c\}$ and $\phi \neq \psi$. Applying this to (10) results in:

$$\mathbb{V}_m\mathbb{V}_m^* = \mathbb{V}_n\mathbb{V}_n^* + \mathcal{H}_{mn} + \dots \\ 2\,\mathbf{Re}\left\{\begin{bmatrix} S_n^a & \gamma_n^{ab}S_n^b & \gamma_n^{ac}S_n^c \\ \gamma_n^{ba}S_n^a & S_n^b & \gamma_n^{bc}S_n^c \\ \gamma_n^{ca}S_n^a & \gamma_n^{cb}S_n^b & S_n^c \end{bmatrix}\mathbb{Z}_{mn}^*\right\}. \tag{11}$$

We now gather the diagonal entries of (11) and place them into a 3×1 vector equation. Defining the variable $y_n^{\phi} = |V_n^{\phi}|^2$, and the vector $\mathbb{Y}_n = \begin{bmatrix} y_n^a, & y_n^b, & y_n^c \end{bmatrix}^T$, (11) becomes:

$$\mathbb{Y}_m = \mathbb{Y}_n + \mathbb{H}_{mn} + \dots \\ 2\,\mathbf{Re}\left\{\begin{bmatrix} (Z_{mn}^{aa})^* S_n^a + \gamma_n^{ab}(Z_{mn}^{ab})^* S_n^b + \gamma_n^{ac}(Z_{mn}^{ac})^* S_n^c \\ \gamma_n^{ba}(Z_{mn}^{ba})^* S_n^a + (Z_{mn}^{bb})^* S_n^b + \gamma_n^{bc}(Z_{mn}^{bc})^* S_n^c \\ \gamma_n^{ca}(Z_{mn}^{ca})^* S_n^a + \gamma_n^{cb}(Z_{mn}^{cb})^* S_n^b + (Z_{mn}^{cc})^* S_n^c \end{bmatrix}\right\}, \tag{12}$$

where $\mathbb{H}_{mn} \in \mathbb{C}^3$ and $\mathbb{H}_{mn}(i) = \mathcal{H}_{mn}(i,i)$ for $i = 1, 2, 3$. Eq. (12) can be restated by grouping the γ and impedance terms into a 3×3 matrix multiplied by a 3×1 vector of complex powers, which results in:

$$\mathbb{Y}_m = \mathbb{Y}_n + \mathbb{H}_{mn} + \dots \\ 2\,\mathbf{Re}\left\{\begin{bmatrix} (Z_{mn}^{aa})^* & \gamma_{ab}(Z_{mn}^{ab})^* & \gamma_n^{ab}(Z_{mn}^{ac})^* \\ \gamma_n^{ba}(Z_{mn}^{ba})^* & (Z_{mn}^{bb})^* & \gamma_n^{ab}(Z_{mn}^{bc})^* \\ \gamma_n^{ca}(Z_{mn}^{ca})^* & \gamma_n^{cb}(Z_{mn}^{cb})^* & (Z_{mn}^{cc})^* \end{bmatrix}\begin{bmatrix} S_n^a \\ S_n^b \\ S_n^c \end{bmatrix}\right\}. \tag{13}$$

Finally, we express the γ terms as generalized complex numbers, $\gamma_n^{\phi\psi} = \alpha_n^{\phi\psi} + j\beta_n^{\phi\psi}$, and organize (13) in terms of active and reactive components $\mathbb{P}_n, \mathbb{Q}_n \in \mathbb{C}^3$:

$$\mathbb{Y}_m = \mathbb{Y}_n + 2\mathbb{M}_{mn}^P\mathbb{P}_n + 2\mathbb{M}_{mn}^Q\mathbb{Q}_n + \mathbb{H}_{mn} \tag{14}$$

where

$$\mathbb{M}_{mn}^P(\phi,\psi) = \begin{cases} r_{mn}^{\phi\psi} & \text{if } \phi = \psi \\ \alpha_n^{\phi\psi}r_{mn}^{\phi\psi} + \beta_n^{\phi\psi}x_{mn}^{\phi\psi} & \text{if } \phi \neq \psi \end{cases} \tag{15}$$

$$\mathbb{M}_{mn}^Q(\phi,\psi) = \begin{cases} x_{mn}^{\phi\psi} & \text{if } \phi = \psi \\ \alpha_n^{\phi\psi}x_{mn}^{\phi\psi} - \beta_n^{\phi\psi}r_{mn}^{\phi\psi} & \text{if } \phi \neq \psi \end{cases} \tag{16}$$

with $a = 1$, $b = 2$, and $c = 3$ for indexing purposes on the LHS of (15) and (16) (e.g. $M_{mn}^P(a,a)$ refers to the (1,1) index). We now re-state (8) for completeness:

$$\mathbb{S}_m = \mathbf{s}_m + \sum_{n:(m,n)\in E}\mathbb{S}_n + \mathbb{L}_{mn}. \tag{17}$$

Eqs. (14) - (17) are a 3-phase representation of the *DistFlow* equations [**?**] which we will henceforth refer to as the *Dist3Flow* equations. In this form, the *Dist3Flow* system reveals an interesting structure of how the ratio of voltages between phases at a given node affects the power/voltage relationship between adjacent nodes. As can be seen in (15) - (16), the ratio of voltages of different phases at the same node are scaling and rotating cross-phase impedances, but do not affect impedances along the main diagonal of a three phase impedance matrix.

Due in part to this interesting relationship, the system of (13) - (17) is nonlinear and non-convex. It is, therefore, difficult to directly incorporate into an OPF formulation without the use of convex relaxations. However, this system can be linearized via making the following assumptions:

- **A1:** $\gamma_n^{\phi,\psi}$ are constant $\forall n \in H$, $\forall \phi \in \{a, b, c\}$, $\psi \in \{a, b, c\}$, $\phi \neq \psi$
- **A2:** $\mathbb{L}_{mn}$ and $\mathbb{H}_{mn}$ are constant $\forall (m, n) \in E$

Application of assumptions **A1** and **A2** to the system of (14) - (17) and (3) results in a linear model that relates the squared magnitudes of nodal voltages and complex power flows to DER injected power. We henceforth refer to the resulting system due to the application of **A1** and **A2** to (14) - (17) as the *LinDist3Flow* equations.

C. LinDist3Flow: Nominal Voltages and No Losses

We now consider a special case for the choice of the constant parameters of **A1** and **A2** and explore the resulting structure of the *LinDist3Flow* equations. Following the analysis presented in [**?**], we neglect the effect of losses in (13) - (17), and choose $\mathbb{L}_{mn} = \mathbb{H}_{mn} = [0, 0, 0]^T$ for all $n \in H$. Next we define the parameter σ such that:

$$\sigma = \frac{-1 + j\sqrt{3}}{2}, \quad \sigma^2 = \frac{-1 - j\sqrt{3}}{2}, \tag{18}$$

and assign them to the γ terms according to:

$$\gamma_n^{ab} = \sigma \quad \gamma_n^{bc} = \sigma \quad \gamma_n^{ac} = \sigma^2 \quad \forall n \in H \tag{19}$$

where clearly $\sigma = 1\angle 120^\circ$ and $\sigma^2 = \sigma^*$. This choice of parameters for **A1** reflects the ratio of nominal voltages at the distribution substation, where, typically, $V_0^a = 1\angle 0^\circ$, $V_0^b = 1\angle 240^\circ$, and $V_0^c = 1\angle 120^\circ$. Choosing the γ terms in this manner fixes the effect of the voltage ratio terms of (15) - (16) to rotating non-diagonal elements of the impedance matrix by $\pm 120^\circ$. With a bit of algebra, it is straightforward to verify that with these choices for **A1** and **A2**, Eqs. (15) - (16) become:

$$\mathbb{S}_m \approx \mathbf{s}_m + \sum_{n:(m,n)\in E}\mathbb{S}_n \tag{20}$$

$$\mathbb{Y}_m \approx \mathbb{Y}_n - \mathbb{M}_{mn}^P\mathbb{P}_n - \mathbb{M}_{mn}^Q\mathbb{Q}_n \tag{21}$$

$$\mathbb{M}_{mn}^P = \begin{bmatrix} -2r_{mn}^{aa} & r_{mn}^{ab} - \sqrt{3}x_{mn}^{ab} & r_{mn}^{ac} + \sqrt{3}x_{mn}^{ac} \\ r_{mn}^{ba} + \sqrt{3}x_{mn}^{ba} & -2r_{mn}^{bb} & r_{mn}^{bc} - \sqrt{3}x_{mn}^{bc} \\ r_{mn}^{ca} - \sqrt{3}x_{mn}^{ca} & r_{mn}^{cb} + \sqrt{3}x_{mn}^{cb} & -2r_{mn}^{cc} \end{bmatrix} \tag{22}$$

$$\mathbb{M}_{mn}^Q = \begin{bmatrix} -2x_{mn}^{aa} & x_{mn}^{ab} + \sqrt{3}r_{mn}^{ab} & x_{mn}^{ac} - \sqrt{3}r_{mn}^{ac} \\ x_{mn}^{ba} - \sqrt{3}r_{mn}^{ba} & -2x_{mn}^{bb} & x_{bc} + \sqrt{3}r_{mn}^{bc} \\ x_{mn}^{ca} + \sqrt{3}r_{mn}^{ca} & x_{mn}^{cb} - \sqrt{3}r_{mn}^{cb} & -2x_{mn}^{cc} \end{bmatrix}. \tag{23}$$

Notice that in the single phase case, the system of (20) - (23) reduces to a variant of the *LinDistFlow* equations.

D. LinDist3Flow: Iterative Approach

When solving an OPF, it is also possible to choose **A1** and **A2** according to an iterative process where these parameters are updated after solving power flow, with control decisions computed during a previous iteration of the OPF. Each re-computation of the constant parameters results in a new set of *LinDist3Flow* equations and the OPF is re-solved until convergence of the updated parameters is achieved. In several experiments, this approach has demonstrated increased accuracy compared to the approach in the previous section. The iterative procedure is executed according to the following steps:

1) Initialize parameters $\gamma_n^{\phi\psi}$, $\mathbb{L}_{mn}$, and $\mathbb{H}_{mn}$. This can be done as was described in section II-C, or by using other constants.
2) Determine control input via solving an OPF using the *LinDist3Flow* equations (i.e. Eqs. (14) - (17) with assumptions **A1** and **A2**).
3) Solve power flow with new control input to calculate $\gamma_n^{\phi\psi}$, $\mathbb{L}_{mn}$ and $\mathbb{H}_{mn}$.
4) Repeat steps 2 and 3 using $\gamma_n^{\phi\psi}$, $\mathbb{L}_{mn}$ and $\mathbb{H}_{mn}$ from previous iteration, until convergence criteria is satisfied.

In Section III-B we demonstrate an OPF formulation that employs this iterative procedure. Future work will addresses mathematical analysis to prove convergence.

III. Simulation Results

In this section, we present two simulation scenarios in which the *LinDist3Flow* equations have been incorporated into OPF formulations. The first experiment considers the dispatch of DER resources to minimize feeder-head real power. The results of the OPF are compared to an alternative optimization approach using convex relaxations and semidefinite programming. The second experiment considers the dispatch of DER resources to regulate and balance feeder voltages.

Both experiments were conducted on the IEEE 13 node distribution feeder model [**?**], the topology of which is shown in Fig. 1. While we have tested both scenarios on larger feeders models, in this work we have chosen to present results for the IEEE 13 node feeder for clarity of presentation and for the large amount of voltage imbalance between phases. In the simulations, feeder topology, line configuration, line impedance, line length, and spot loads are specified in [**?**]. Delta to Wye conversions were performed where appropriate. Furthermore, our simulations omitted the voltage regulator between nodes 650 and 632, the transformer between nodes 633 and 634, the switch (assumed closed) between nodes 671 and 692, and capacitors at nodes 675 and 611. Spot loads were increased by a factor of 1.25 to increase voltage imbalance. Finally, four-quadrant-capable DER were placed at the following nodes: 632, 675, 680, and 684. We assume each DER has 3 phase control and can inject or sink both real and reactive power separately on each phase of the feeder. The DER are constrained by an apparent power capacity limit

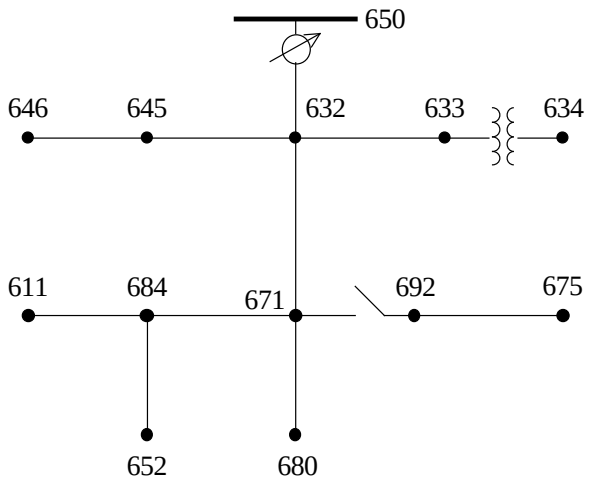

Fig. 1: IEEE 13 node feeder model.

on each phase of 250 kVA, or 0.05 pu. In both experiments, voltage magnitudes were constrained to be within $\pm 5\%$ of 1.0 p.u. The voltage at the feeder head was assigned as: $\mathbb{V}_0$ = $[1\angle 0°,\ 1\angle 240°,\ 1\angle 120°]^T$ p.u. for phases a, b, and c, respectively.

Figure 2 shows the feeder voltage magnitude profile without any applied control (i.e. this is the "no control" scenario in both experiments). In this and all subsequent figures, phase a is depicted in red, phase b is depicted in green, and phase c is depicted in blue. Fig. 2 highlights the large amount of voltage magnitude imbalance as well as violations of minimum voltage magnitude constraints on phase c.

A. Minimization of Feeder Real Power Scenario

The goal of this experiment was to test the effectiveness of the *LinDist3Flow* model in an OPF formulation, with **A1** - **A2** applied to (14) - (17) as outlined in Section II-C (resulting in Eqs. (20) - (23)) . The objective of the OPF was to control DER real and reactive power resources to minimize feeder head real power, subject to voltage magnitude and DER inverter capacity constraints.

Minimization of feeder head real power was chosen as the objective of (24) as it is possible to compare results to those determined via convex relaxation techniques and semidefinite programming, outlined in [**?**] - [**?**] (we henceforth refer to these results as "SDP"). In this scenario, we assumed constant power loads where $a_{0,n}^{\phi} = 1$ and $a_{1,n}^{\phi} = 0\ \forall n \in H$. We define the OPF that employs the *LinDist3Flow* model as:

$$\begin{aligned} \underset{u_n^\phi, v_n^\phi, y_n^\phi, P_n^\phi, Q_n^\phi}{\text{minimize}} \quad & \sum_{\phi\in\{a,b,c\}} P_0^\phi \\ \text{subject to} \quad & (20)-(23), \quad \underline{y} \le y_n^\phi \le \overline{y}, \\ & \left|w_n^\phi\right| \le \overline{w}, \quad \forall n \in H \end{aligned} \tag{24}$$

A comparison between the SDP and the OPF of (24) is shown in Fig. 3, with Fig. 3a showing the voltage magnitude profile using the SDP optimal control (note that the SDP achieved a rank 1 solution), and Fig. 3b showing the voltage magnitude profile obtained from applying control inputs determined from (24). Though there is a visible difference

in the voltage profiles derived in each case, both control formulations deployed DER resources to bring voltages to within acceptable limits. Interestingly, while the optimal control given by the SDP and (24) had the same real parts (DER real power output), the imaginary parts (DER reactive output) were different, leading to different voltage magnitudes. The optimal cost, computed as $\sum_{\phi\in\{a,b,c\}} P_0^\phi$, was 0.83732 p.u. for the uncontrolled case, 0.27634 p.u. for the SDP case, and 0.27688 p.u. for the case of (24), a difference of 0.2 %.

B. Voltage Balancing Scenario

We now present the results of our second experiment, in which we incorporated two realizations of the *LinDist3Flow* equations into OPFs that used DER resources to regulate and balance voltage magnitudes on an unbalanced radial distribution feeder. Voltage balancing is an important objective as many three phase loads (induction motors for instance) are sensitive to high levels of imbalance. Furthermore, many 3-phase voltage regulation equipment actuates based solely on single phase measurements. Therefore, significant levels of imbalance can lead to improper operation of these devices.

The results in this section expand on our previous work in [**?**] via adopting the iterative approach outlined in Section II-D. This simulation incorporated both constant power and constant impedance loads as defined in [**?**] for the 13 node case. We define the problem as:

$$\begin{aligned} \underset{u_n^\phi, v_n^\phi, y_n^\phi, P_n^\phi, Q_n^\phi}{\text{minimize}} \quad & \sum_{n\in H}\left[\sum_{\phi\neq\psi}(y_n^\phi - y_n^\psi)^2 + \rho\sum_{\phi}\left|w_n^\phi\right|^2\right] \\ \text{subject to} \quad & (14)-(17), \quad \underline{y} \le y_n^\phi \le \overline{y}, \\ & \left|w_n^\phi\right| \le \overline{w}, \quad \forall n \in H \end{aligned} \tag{25}$$

where $\phi, \psi \in \{a, b, c\}$. The parameter ρ was chosen as 0.01 and is a penalty on control action. We compared three cases to investigate the benefit of the iterative algorithm of Section II-D, as listed below:

- Case 0 - The uncontrolled, or base case (see Fig. 2).
- Case 1 - OPF initialized as per assumptions outlined in Section II-C with $\gamma_n^{\phi\psi} = \sigma$ or σ^2, and $\mathbb{L}_{mn} = \mathbb{H}_{mn} = 0_{3\times1}$. See Fig. 4a
- Case 2 - OPF solved as outlined in Section II-D. See Fig. 4b

It should be noted that comparison of either case to an SDP formulation of (25) was not possible as it is not, to the authors knowledge, possible to formulate a semidefinite program with this objective function.

It can clearly be seen that for both Case 1 and Case 2, the voltage imbalance is drastically reduced compared to Case 0. In Case 1, the gap between phases a and b is reduced, however the magnitude of phase c remains lower throughout the feeder. In Case 2, the three phases are much more closely matched. We define voltage imbalance for the network as:

$$J(\mathbb{Y}) = \sum_{n\in H}\sum_{\phi\neq\psi}(y_n^\phi - y_n^\psi)^2 \tag{26}$$

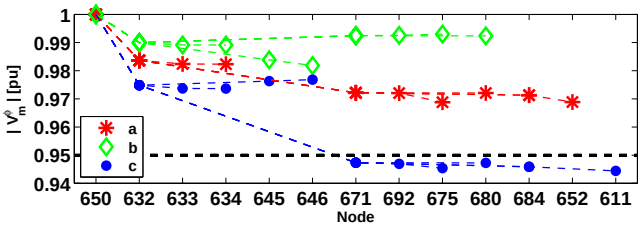

Fig. 2: Voltage profile of IEEE 13 node feeder with zero control.

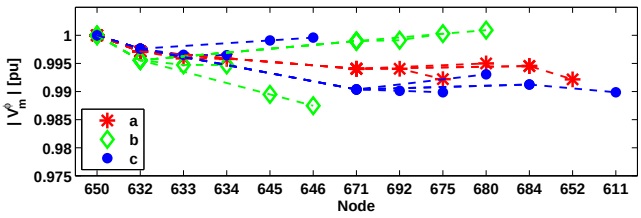

(a) Voltage profile of IEEE 13 node feeder with SDP control.

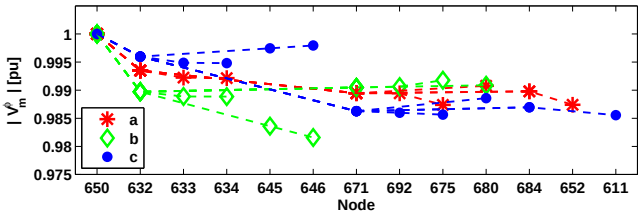

(b) Voltage profile of IEEE 13 node feeder with control from (24)

Fig. 3: Comparison of voltage profiles for feeder head real power minimization scenario.

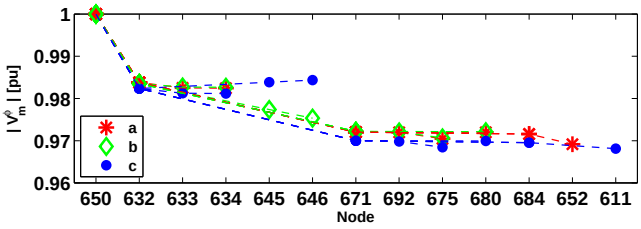

(a) Voltage profile of IEEE 13 node feeder with (25) Case 1 control.

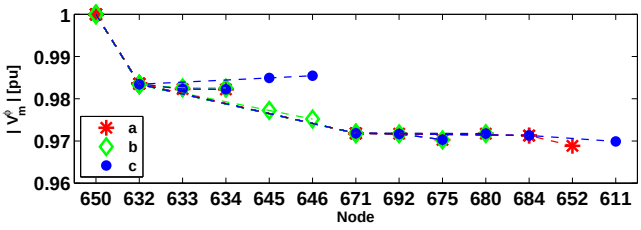

(b) Voltage profile of IEEE 13 node feeder with (25) Case 2 control.

Fig. 4: Comparison of voltage profiles for voltage balancing scenario.

where $\phi, \psi \in \{a, b, c\}$ and $\mathbb{Y}$ is the set of all $\mathbb{Y}_n$, $n \in H$. The voltage imbalance for Case 0 is 0.05443. The imbalance for Case 1 is 8.334e-4, and the imbalance for Case 2 is 8.054e-4, a 3.36 % improvement over Case 1.

IV. Conclusion

Optimization of unbalanced power flow is a challenging topic due to its nonlinear and non-convex nature. While

recent works on SDP relaxations [**?**] - [**?**] have made OPF formulations for unbalanced systems possible, these approaches suffer from restrictions on the possible objectives and a high-dimensional geometrical complexity that impedes feasibility and uniqueness of the solutions. In an effort to solve problems that cannot be addressed via SDP techniques, in this paper we sought to develop an approximate model for distribution power flow that could be subsequently incorporated into optimal power flow problems.

To do so, we derived a generalized model of distribution system power flow that maps real and reactive power injections into squared voltage magnitude differences. The resulting model, which we referred to as the *Dist3Flow* equations, can be viewed as an extension of the *DistFlow* [**?**] equations to 3-phase unbalanced distribution systems. As the *Dist3Flow* model is nonlinear and not necessarily convex, we suggested two procedures to linearize the system into a form suitable for incorporation into OPF formulations. The linearized power flow model, which we have referred to as the *LinDist3Flow* system, is obtained by approximating the nonlinear components of the original equations.

The first approximation procedure treated the ratio of voltages of different phases as a constant and neglected line losses. The resulting *LinDist3Flow* system was tested in an OPF with the objective of minimizing feeder-head real power. Comparison of results obtained to a SDP formulation of the same problem revealed that the OPF driven by the *LinDist3Flow* model achieved a solution whose objective function was within 0.2% of the optimal value. The second procedure for approximating the *Dist3Flow* equations involved iterating over the nonlinear terms between successive runs of solving the power flow equations and then solving the OPF. This approach was simulated in an OPF formulation with the objective of regulating and balancing system voltages, and was shown to increase accuracy compared to the previous approximation technique.

Although it is an approximation, the principle advantage of *LinDist3Flow* model is that it enables an optimal power flow schemes where the constraints are linear and convex relaxations are not required. As such, for strictly convex objectives with a non-empty feasible set, the OPF will always find an optimal solution to the approximate problem. As was mentioned previously, an OPF driven by the *LinDist3Flow* model was able to solve a voltage balancing optimization, for which, by the knowledge of the authors, a SDP formulation does not exist. Although the final solution is only approximate. The iterative method shows potential for further improving the accuracy gap between the linear and full nonlinear model, and future work will consider mathematical analysis to characterize this.

The feasibility of the *LinDist3Flow* model can be exploited in OPF formulations with a variety of relevant objectives, such as voltage balancing, loss minimization, or economic dispatch. Our future work is aimed at exploring other useful applications of three phase unbalanced OPF such as voltage reference tracking or battery and electric vehicle charging. First, we will use our findings to extend the authors' work on optimal decentralized voltage regulation [**?**], developed for single-phase balanced networks, to 3-phase unbalanced systems. Furthermore, in a recent work, the authors developed a framework for distribution grid state estimation with limited sensing and forecasting information, using linearized power flow equations for single-phase systems [**?**]. We aim to extend these results to unbalanced systems using the *LinDist3Flow* equations.

REFERENCES

[1] E. M. Stewart, S. V. MacPherson, D. Nakafuji, and T. Aukai, "Analysis of high-penetration levels of photovoltaics into the distribution grid on oahu, hawaii, detailed analysis of heco feeder wf1," NREL subcontract report NREL/SR-5500-54494, Tech. Rep.

[2] "Voices of experience - insights into advanced distribution management systems," 2015. [Online]. Available: https://www.smartgrid.gov/document/insights_advanced_distribution_management_systems.html

[3] K. Turitsyn, P. Sulc, S. Backhaus, and M. Chertkov, "Options for control of reactive power by distributed photovoltaic generators," *Proceedings of the IEEE*, vol. 99, no. 6, pp. 1063–1073, 2011.

[4] N. Li, G. Qu, and M. Dahleh, "Real-time decentralized voltage control in distribution networks," in *Communication, Control, and Computing (Allerton), 2014 52nd Annual Allerton Conference on*. IEEE, 2014, pp. 582–588.

[5] B. Robbins, C. N. Hadjicostis, A. D. Domínguez-García *et al.*, "A two-stage distributed architecture for voltage control in power distribution systems," *Power Systems, IEEE Transactions on*, vol. 28, no. 2, pp. 1470–1482, 2013.

[6] B. Zhang, A. D. Dominguez-Garcia, and D. Tse, "A local control approach to voltage regulation in distribution networks," in *North American Power Symposium (NAPS), 2013*. IEEE, 2013, pp. 1–6.

[7] M. Farivar, C. R. Clarke, S. H. Low, and K. M. Chandy, "Inverter var control for distribution systems with renewables," in *IEEE International Conference on Smart Grid Communications (SmartGridComm)*. IEEE, 2011, pp. 457–462.

[8] A. Lam, B. Zhang, A. Dominguez-Garcia, and D. Tse, "Optimal distributed voltage regulation in power distribution networks," *arXiv preprint arXiv:1204.5226*, 2012.

[9] M. E. Baran and F. F. Wu, "Optimal sizing of capacitors placed on a radial distribution system," *IEEE Transactions on Power Delivery*, vol. 4, no. 1, pp. 735–743, 1989.

[10] W. H. Kersting, *Distribution system modeling and analysis*. CRC press, 2012.

[11] E. Dall'Anese, G. B. Giannakis, and B. F. Wollenberg, "Optimization of unbalanced power distribution networks via semidefinite relaxation," in *North American Power Symposium (NAPS), 2012*. IEEE, 2012, pp. 1–6.

[12] E. Dall'Anese, H. Zhu, and G. Giannakis, "Distributed optimal power flow for smart microgrids," *Smart Grid, IEEE Transactions on*, vol. 4, no. 3, pp. 1464–1475, 2013.

[13] R. Louca, P. Seiler, and E. Bitar, "Nondegeneracy and inexactness of semidefinite relaxations of optimal power flow," *arXiv*, vol. 1441.4663v1, 2014.

[14] D. B. Arnold, M. D. Sankur, R. Dobbe, K. Brady, D. S. Callaway, and A. Von Meier, "Optimal dispatch of reactive power for voltage regulation and balancing in unbalanced distribution systems," *IEEE Power and Energy Society General Meeting, accepted*, 2016.

[15] "IEEE Distribution Test Feeders," http://ewh.ieee.org/soc/pes/dsacom/testfeeders/index.html, [Online; accessed May-2015].

[16] O. Sondermeijer, R. Dobbe, D. Arnold, C. Tomlin, and T. Keviczky, "Regression-based inverter control for decentralized optimal power flow and voltage regulation," in *Power & Energy Society General Meeting*. IEEE, 2016.

[17] R. Dobbe, D. Arnold, S. Liu, D. Callaway, and C. Tomlin, "Real-time distribution grid state estimation with limited sensors and load forecasting," in *International Conference on Cyber-Physical Systems*. ACM/IEEE, 2016.